Numerical Analysis of a ITO Based Circularly Polarized Optically Transparent THz Antenna Employing Characteristic Mode Analysis

Muhammad Asad Rahman[1, *], Md. Sarwar Uddin Chowdhury[1], Md. Azad Hossain[1], and Ahmed Toaha Mobashsher[2]

Abstract—An optically transparent circularly polarized indium tin oxide (ITO) based antenna having operability in THz region is proposed in this paper. An E-shaped slot and an I-shaped slot are embedded into an E-shaped radiating patch modeled by ITO and conductive carbon nanotube (CNT) on a polyimide substrate to obtain circular polarization. The unequal parallel slits of the E-shaped patch with an E-shaped slot lead to introduce two orthogonal modes, and hence circular polarization is achieved. Besides, integration of an I-shaped slot also helps to create the difference in magnitude of current distribution between the two working modes to get better axial ratio. The patch of the antenna is covered with highly CNT film which improves the overall performance of the antenna. To overcome the limitations of the traditional design process, characteristic mode analysis is carried out which helps to realize and analyze circular polarization generation mechanism effectively. The proposed antenna shows a wide 3-dB axial ratio bandwidth of 9.66%. A reasonable gain of 2.61 dBic is obtained at 1.11 THz with excellent radiation performance. Wide 3-dB axial ratio bandwidth with reasonable gain makes this light weight transparent small-antenna competent for wireless and satellites applications.

1. INTRODUCTION

In recent years, a large number of applications are transferring from stationary computer to wireless devices such as smart phones due to portability and real time use [1]. This creates high data traffic with lack of bandwidth resources. Moreover, current communication system is not adequate to meet the exploding data rate requirements of an ultra-wide bandwidth communication network [2]. Therefore, to satisfy the needs of applications and devices demanding high speed data transmission, the use of THz frequency band (0.1–10 THz) can be a suitable solution.

Antenna is a critical component to support THz systems. Conductive materials such as copper (Cu), gold (Au), and dielectric materials such as FR4 and Teflon used for low frequency antennas are not suitable for designing THz antennas due to high loss and lack of efficiency. As nanotechnology continues to improve quickly, antennas designed by conductive thin films for THz band rather than conventional design materials like Cu, Au, etc. are increased at a high rate. Conductive films like transparent conductive oxides (TCO), nanocarbon (carbon nanotubes, graphene), metallic nanostructure (thin metal films, metallic nanowires, and patterned metal grids), and conductive polymers are utilized to design novel antennas. There are different TCO materials namely Indium Tin Oxide (ITO), Fluorine Tin Oxide (FTO), Silver Tin Oxide (AgHT-8), etc. Among them, ITO thin film is mainly utilized in designing optically transparent antennas (OTA) for its best tradeoff between electrical conductivity and optical transmittance. In industries, ITO is mostly used with a sheet resistance of $30\,\Omega/\text{sq.}$ to $80\,\Omega/\text{sq.}$ and optical transmittance of 90% [3]. However, ohmic losses in the ITO sheet causes the degradation of the

overall performance of the antenna. To overcome this limitation and improve the overall performance, highly conductive material like carbon nanotube (CNT) can be coated over the ITO patch. It has been studied for various chemical as well as physical properties and applications. CNTs are tubes of carbon particles in nanoscale with exceptional characteristics. These characteristics include high electrical conductivity and optical transparency, easy fabrication process, flexibility, and stronger mechanical strength [4].

OTAs have been continuously developed for integrating with solar cells, displays, vehicular communications, and ultra-high speed communication in recent years. In satellites applications, OTA is used in integration with solar cell as it helps to overcome the limitations of space constrains and mismatch in solar panel due to the shadow of the conventional nontransparent antenna for which efficiency of the cell is degraded. In addition to integration with solar cell, OTAs can also be used in satellites by placing it on optical displays and heat reflecting transparent mirrors [5]. This type of antennas can also provide wide bandwidth (BW) facility as compared to conventional antennas which is another essential factor for satellite communications. The first OTA made of an AgHT-8 optically transparent conductive coating on a clear thin polyester sheet was developed by Simons and Lee in 1997 [6]. Since then, diverse works on designing OTAs of different shapes with optically transparent conductive materials have been reported from time to time [7–9]. But many of the OTAs have some limitations like low fractional impedance BW ($< 5\%$), poor gain ($< 2\,\mathrm{dBi}$), and poor radiation efficiency [10]. In order to make the antennas optically transparent by utilizing optically transparent conductive materials, one has to confront several limitations of the materials itself like skin depth losses, ground-effect losses, and high resistivity losses [11].

Some works on OTAs such as ITO and FTO based U-shaped antenna [12], FTO based E-shaped antenna [5], ITO based E-shaped antenna [13], graphene based rectangular patch antenna [14], AgHT-8 based CPW-fed antenna [15, 16], and AgHT-8 based antenna with rectangular branches [17] have been reported until now. These antennas provide the advantage of wide BW. However, they are basically linearly polarized. The primary idea to generate circular polarization (CP) is to excite two orthogonal nearly degenerate modes where the quadrature phase shift is present between the two modes. A meshed type circularly polarized OTA has been reported in [18] for K-band applications which provides a gain of nearly $4\,\mathrm{dBic}$, but the 3-dB AR BW remains narrow. In [19], an AgHT-4 laminated CP OTA for $5.8\,\mathrm{GHz}$ WLAN applications has been reported which provides somewhat improved BW, but the gain remains very low ($0.92\,\mathrm{dBic}$).

Though there are several techniques for CP antenna design [20–22], none of them can provide insightful physical information of the antenna. Characteristic mode analysis (CMA) is a better solution to overcome these limitations as it provides better understanding of the antennas working principles and operations including CP generation mechanism with the help of different current modes. It helps to optimize the antenna structure for obtaining optimum performance.

The characteristic mode theory (CMT) was first launched by Garbacz and Turpin in 1970s [23]. Later a distinct technique to apply the CMT to metallic [24], dielectric, and magnetic structures [25–34] was reported by Harrington et al. After that, CMA based on CMT has gained a great momentum to design different antennas and explain their operation mechanism properly [26–30].

In this paper, a newly configured E-shaped wideband ITO-based CNT coated antenna resonating at $1.12\,\mathrm{THz}$ is presented. Though there are a lot of research works done so far on CP antenna in GHz region, but in THz region, it is still in initial stage. Besides, though ITO and CNT are used to design THz antenna, previous woks are not essentially done on E-shaped CP antenna. So, the proposed E-shaped CP antenna designed by embedding E-shaped and I-shaped slots and covered with CNT with wide 3-dB axial ratio (AR) BW is totally novel for THz region. Better CP performance is possible to achieve due to the unequal slits length of E-shaped patch along with E-shaped and I-shaped slots. An RHCP structure has been proposed by the authors in [31], but no analysis of the antenna was done. Therefore, for the first time parametric study is done by CMA instead of conventional parametric analysis to optimize an OTA structure which helps to determine the physical insight of the antenna by reducing optimization time considerably. Design and performance analysis of the proposed antenna along with elaborate CMA analysis as well as a comparison with some previous standard works on OTAs are demonstrated in the following sections.

2. PROPOSED ANTENNA

2.1. Structure

Figure 1 shows the geometry of the proposed wideband E-shaped CP OTA along with cross sectional view (AA′). E-shaped radiating patch and ground are modeled using a $0.40\,\mu m$ thick transparent ITO thin film. Optical transmittance of ITO film is greater than 90% with an electrical resistivity of $7.2 \times 10^{-4}\,\Omega$-cm [32]. A $20\,\mu m$ thick polyimide film as a substrate having dielectric constant of 3.5 and loss tangent of 0.008 is sandwiched between the patch and ground plane. Polyimide is well known for thermal stability ($> 500°C$), chemical resistance, and mechanical strength [33]. It also shows excellent dielectric properties and inherently low coefficient of thermal expansion with optical transmittance of more than 86% in visible light [34]. The E-shaped patch of length L_P and width W_P contains two slits (Slit-1 and Slit-2 in Figure 1) having different lengths of L_1 and L_2 ($L_1 < L_2$) with the same width of W_S. An E-shaped slot with unequal arms and an I-shaped slot are embedded into the E-shaped patch. The E-shaped slot is placed between the two slits of the E-shaped patch. The length and arm widths of the embedded E-shaped slots are h, E_1, E_2, and E_3, respectively with the same slot width of E_S. The embedded I-shaped slot, which is located on the top right corner of the E-shaped patch, has the dimension of $L_{SI} \times W_{SI}$. Finally, the ITO patch is covered with a CNT thin film of thickness $0.20\,\mu m$. CNT film shows high electrical conductivity of $2 \times 10^7\,S/m$ that is close to metal [4, 35], and this high electrical conductivity of CNT associated with ITO improves the overall performance of the proposed antenna. Moreover, the CNT film exhibits optical transmittance of 80–90% [36]. In the proposed design, the dimension of the CNT coating is the same as patch except the length of the two slits of the E-shaped patch. The two slits of CNT cover have the lengths of $(L_1 - X_1)$ and $(L_2 + X_2)$. The unequal slits lengths of E-shaped patch along with integrated E- and I-shaped slots help to vary the current distributions of the two modes and thus contribute to achieving CP. The difference in lengths
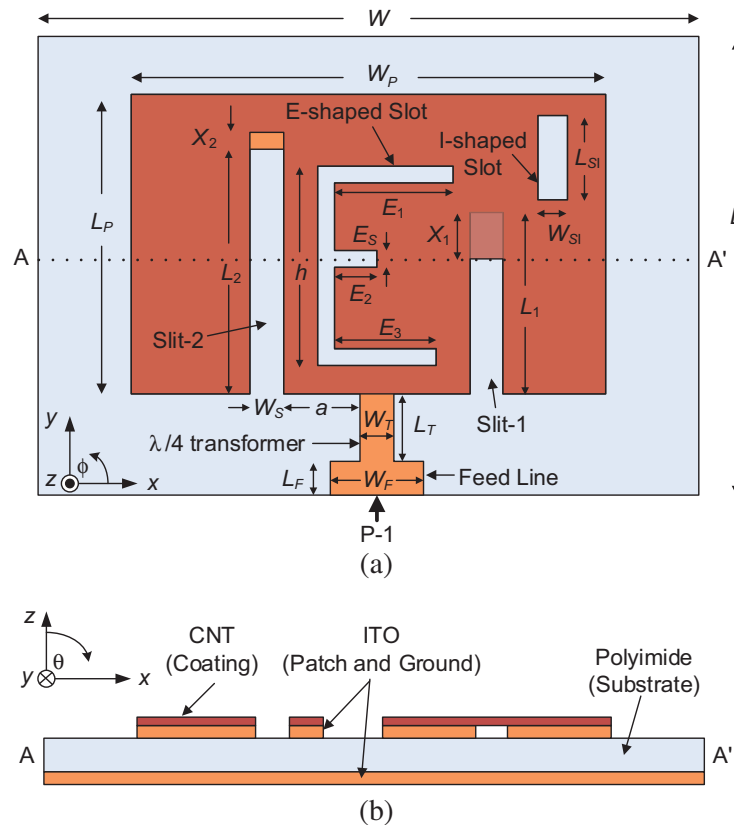

Figure 1. Geometry of the proposed E-shaped CP OTA, (a) top view, (b) cross sectional view (AA′). [This figure is not drawn to scale].

of the two slits of the E-shaped patch and coating also supports to adjust the current magnitude of the two modes and thus contribute to improve the AR of the antenna. A feed line consists of a series connected 50-Ω line and $\lambda/4$ transformer having dimensions $L_\mathrm{F} \times W_\mathrm{F}$ and $L_\mathrm{M} \times W_\mathrm{M}$, respectively, which is used to excite the antenna using a waveguide port, P-1. The optimized dimensions of the designed wideband OTA are tabulated in Table 1.

Table 1. Parameters and optimum dimensions of the proposed wideband OTA.

Variable	L	W	L_1	L_2	W_S	h	E_1	E_2	E_3	E_S
Dimensions (μm)	150	300	40	53	6	45	27	13	25	3
Variable	L_P	W_P	L_SI	W_SI	X_1	X_2	L_F	W_F	L_T	W_T
Dimensions (μm)	70	100	15	5	10	6	15	46	25	14

2.2. Outline of Manufacturing Process

Antenna design techniques used for lower frequencies are equally applicable to THz whereas the antenna fabrication process for THz is quite complex [2]. Copper is used as a material of radiating and ground layers for antennas operating at lower RF frequencies. Hence, the design of antenna can be realized on a printed circuit board (PCB) having double sided copper layer by employing PCB milling machine, laser cutting, or photoengraving technique. However, in the case of THz frequency, copper is not a suitable material for antenna, as radiation efficiency of the antenna is reduced due to the decrease of skin depth and conductivity of copper [37]. Therefore, the selection of appropriate materials with minimum losses and suitable fabrication technique are a significant task for realizing THz antennas.

In this article, the proposed design contains three transparent materials: ITO and CNT as conductive material and polyimide as substrate. The thin film of these materials can be deposited using a variety of deposition methods such as chemical vapor deposition (CVD), drying from solvent, pulsed laser deposition, sputtering, etc. However, these deposition processes are not suitable to realize different shapes of the antenna. Considering this difficulty of fabrication, ink-jet printing process [38–43] can be employed to fabricate the proposed antenna. Polyimide thin film is available as a flexible sheet for industrial applications. It can be used as a substrate to realize the antenna. To make the conducting layers on polyimide film, ITO ink [44] can be ink-jet printed on the both sides of the polyimide film [45]. After that, on the radiating patch side, CNT conductive ink [46] can be used to print the CNT layer on the ITO layer [47]. On the other hand, considering the frequency of the proposed antenna, THz-wave photomixer module is suitable for signal input. Uni-traveling-carrier photodiode (UTC-PD) mixer module such as IOD-PMAN-13001 developed by NTT, Japan [48] which operates up to a frequency of 2.5 THz can be integrated with the proposed antenna to excite it by THz signal.

3. CHARACTERISTIC MODE ANALYSIS OF THE PROPOSED OTA

CMT is a physics based deterministic process, which has found many applications in the fields of radiator design, radiated emission analysis, and electromagnetic interference modeling. CMA is a CMT based source free process of describing the characteristics of arbitrary shaped radiating bodies by calculating a weighted set of orthogonal current modes. These current modes of an arbitrary radiating structure can be found by resolving the following highly weighted equation [49]:

$$X\left(\overline{J}_\mathrm{n}\right) = \lambda_\mathrm{n} R\left(\overline{J}_\mathrm{n}\right) \tag{1}$$

where $\overline{J}_\mathrm{n}$ are real eigenvectors or eigen currents; λ_n are real vector eigenvalues; R and X are real and imaginary parts of Hermitian impedance matrix $Z = R + jX$.

These current modes not only make the modal analysis feasible but also reveal necessary information for antenna design which includes: the dominant modes and excited modes for wideband operation, the center frequencies of all considered modes, physical insight of how the structure radiates, surface current

distributions of all modes of the structure, and significance of the modes at a particular frequency. Since CMA is an excitation free process, characteristic modes behavior only depends on the shape and size of radiating structure. CMA facilitates step-by-step advancement of the antenna design rather optimizing the structure at a time. The following steps are followed for optimizing the structure using CMA. First, optimizations of the size and shape of radiating structure are done. Once size of the structure is scaled, then resonant frequency of the modes can be modified by varying the shape of the structure which causes varying the radiation characteristics of the modes. Next, a proper feeding arrangement is chosen so that the desired modes can be excited. Small radiating structure can be effectively modeled by considering a few modes. Thus, it is possible to design small and intermediate-size antennas in a wideband range by taking only four or five characteristic modes into account.

To apply CMT to a given structure, the proper selection of significant modes is an essential requirement for the correct conclusion of the resultant fields. In the case of CP, the significant modes can be determined by analyzing two parameters namely modal significance and characteristic angle, and finally verified by a third parameter namely eigenvalue. For the ease of description at first details regarding eigenvalue are discussed.

Eigenvalue (λ_n) is used to provide the assurance that the correct modes are selected for CP generation by observing the value for two orthogonal modes. λ_n varies in the range of $-\infty$ to ∞. The total field energy stored within a scattering or radiating body is proportional to the magnitude of the eigenvalue. For a certain mode, if $\lambda_n = 0$ at a certain frequency, the mode is at resonance at that frequency. If $\lambda_n > 0$, the mode stores magnetic energy and is known as inductive mode. On the other hand, the mode stores electrical energy, if $\lambda_n < 0$, and is known as capacitive mode. However, for CP, the eigenvalues of the two modes are required to be checked. If the eigenvalue of one mode is equal and opposite to the eigenvalue of another mode, in that case the capacitive energy stored by one mode is cancelled by magnetic energy stored by another mode. As a result, these two modes satisfied the resonance condition, and CP can be achieved by exciting these two modes.

Modal significance (MS_n) is the intrinsic feature of each mode and independent of external excitation. It measures the contribution of each current mode in the whole electromagnetic response to an external excitation and can be defined by following equation:

$$MS_n = \left| \frac{1}{1 + j\lambda_n} \right| \tag{2}$$

Besides, the BW of each current mode, particularly when a specific feeding arrangement is not available in the initial stage of designing, can be determined by modal significance. According to MS_n, a half power BW is defined as:

$$\text{BW} = \frac{f_H - f_L}{f_{\text{Res}}} \tag{3}$$

where f_L, f_H, and f_{Res} are lower band frequency, upper band frequency, and resonant frequency, respectively.

$$MS_n\left(f_{\text{Res}}\right) = 1 \tag{4}$$

$$MS_n\left(f_H\right) = MS_n\left(f_L\right) = \left| \frac{1}{1 + j\lambda_n} \right| = 1/\sqrt{2} \tag{5}$$

It is possible to determine the significant and non-significant modes with the help of MS_n. If $MS_n \geq 1/\sqrt{2}$ for a mode, the mode is considered as a significant mode, while if $MS_n < 1/\sqrt{2}$ for a mode, the mode is considered as a non-significant mode. This criterion helps to omit higher order modes without affecting the approximation of designed radiation pattern. Generally, two significant modes with the same modal significances are excited simultaneously for achieving a CP antenna. The smooth changes of MS_n with the frequency ensure that the sized radiation patterns are stable within a reasonable frequency band.

Characteristic angle (α_n) provides a way to better show the mode behavior near resonance frequency. It models the phase difference between the characteristic current $\overline{J}_n$ and its associated characteristic field $\overline{E}_n$, and is defined by $\alpha_n = 180° - \tan^{-1}(\lambda_n)$. The change of α_n with frequency gives qualitative information to describe the radiation or scattering capability of each mode. More specifically,

the phase information in α_n helps to determine whether two orthogonal modes can be excited with one feeding for CP antenna design.

More often, α_n varies in the range of 90° to 180°. In the current case, two orthogonal modes with comparable modal significance and 90° characteristic angle difference are required for satisfactory AR performance.
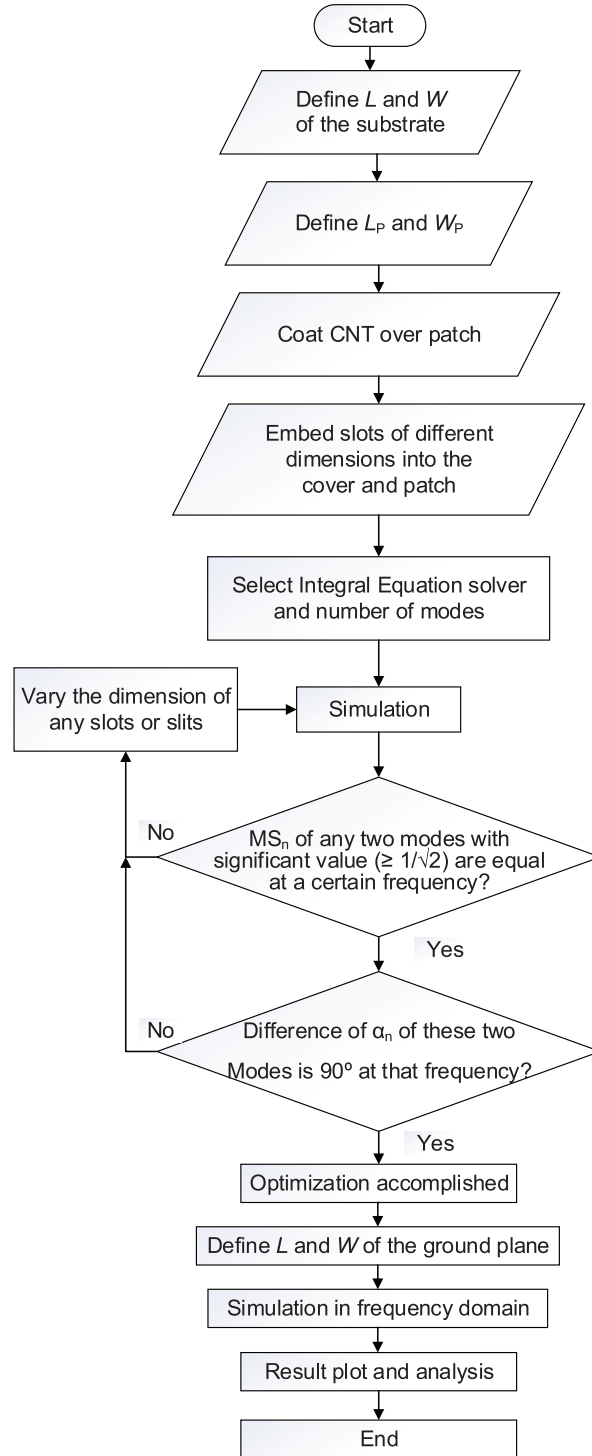

Figure 2. Flow chart describing the design process of the wideband CP OTA utilizing CMA.

If $\alpha_n = 180°$, the corresponding modes are resonant modes.

If $90° < \alpha_n < 180°$, the corresponding modes are inductive modes.

If $180° < \alpha_n < 270°$, the corresponding modes are capacitive modes.

So for a CP antenna, one inductive mode and one capacitive mode are needed to be excited simultaneously. So, the requirements of these two modes are:

1. The modal current distribution of one mode in terms of either polarization or magnitude requires to be orthogonal to the other mode.

2. $MS_n \geq 1/\sqrt{2}$ and $MS_1 = MS_2$ at a certain frequency.

3. One inductive mode and one capacitive mode with $45°$ apart from $180°$ are needed to be excited simultaneously, i.e., characteristic angle of inductive mode should be $135°$, and characteristic angle of capacitive mode should be $225°$.

4. λ_n corresponding to these two modes require to be equal and opposite in magnitude.

The flowchart of the proposed OTA design process utilizing CMA is illustrated in Figure 2.

Modal significance (MS_n) curves corresponding to the first five modes are plotted in Figure 3(a). The values of MS_n provide the information regarding selection of probable modes which contribute to generate CP and the associated resonant frequencies. It is obvious that mode 1 and mode 2 intersect each other at 1.09 THz and 1.12 THz with MS_n of 0.98 and 1.00, respectively. MS_n of mode 1 and mode
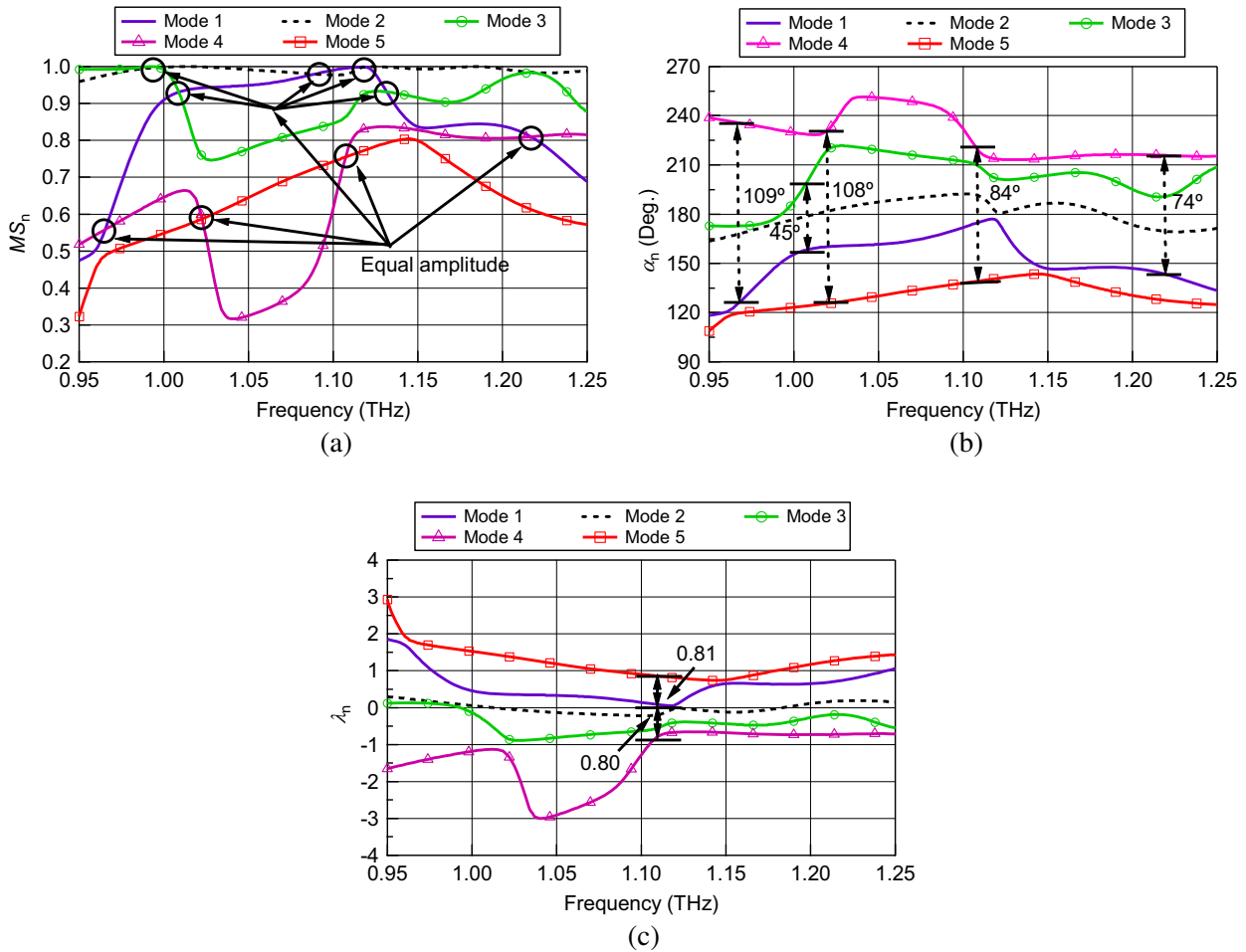

Figure 3. MS_n, α_n, λ_n curves correspond to the first five modes of the proposed OTA. (a) Modal significance (MS_n). (b) Characteristic angle (α_n). (c) Eigenvalue (λ_n).

3 are found the same at 1.01 THz ($MS_n = 0.93$) and 1.13 THz ($MS_n = 0.92$). Mode 2 and mode 3 have the same MS_n of 1.00 at 1.09 THz and 0.98 at 1.12 THz. Moreover, mode 1 and mode 4 have equal MS_n of 0.55 and 0.82 at 0.97 THz and 1.22 THz, respectively. It is seen that at 0.97 THz, MS_n is less than $1/\sqrt{2}$. So this option needs not to be considered further. For mode 4 and mode 5, it is seen that they cross each other at 1.02 THz and 1.11 THz with MS_n of 0.59 and 0.76. It is obvious that at 1.02 THz, MS_n is less than $1/\sqrt{2}$. Hence, this frequency will not be considered more. For other frequencies, the values of α_n need to be explored.

Characteristic angle (α_n) curves of the first five modes are depicted in Figure 3(b). The value of α_n helps to reduce the number of probable resonant frequencies and resonating modes considered so far. It is seen from the figure that the maximum difference of α_n between mode 1 and mode 2 is 55° at 0.95 THz, and both the modes are inductive modes. So the frequency associated with mode 1 and mode 2 with same MS_n will not be taken into account further. For mode 2 and mode 3, it is also obvious that the highest difference of α_n is 40° at 1.02 THz, and both the modes are capacitive modes. Therefore, the frequency corresponding to these two modes with same MS_n needs not to be regarded more. For mode 1 and mode 4, it is clear that the difference of α_n at 1.22 THz is 74° which is not close enough to 90° to be considered. On the other hand, for mode 4 and mode 5, it is seen that at 1.11 THz the difference of α_n is 84° where both the modes are 42° apart from 180°. So far, only mode 4 and mode 5 satisfy the condition of achieving CP performance.

Figure 3(c) shows the variation of eigenvalues (λ_n) over frequency of the first five modes. With the help of λ_n, the modes selected by utilizing MS_n and α_n for generating CP can be verified. From the plot, it is obvious that at 1.11 THz, λ_n corresponding to mode 4 is -0.80 while λ_n corresponding to mode 5 is 0.81. So if mode 4 and mode 5 can be excited simultaneously at 1.11 THz, it is possible to get better CP performances.

Surface current distributions of mode 4 and mode 5 are depicted in Figure 4. The two modes will be orthogonal to each other if the current distributions of these two modes will satisfy one of the following two points [50]

1. There exist orthogonality in terms of current polarizations of the two modes to be excited.
2. There exists orthogonality in terms of current magnitudes of the two modes to be excited.

For the second case, if current distribution of one mode is very intense at a certain point of the surface, then its orthogonal current mode must have very poor modal current at that particular surface point. From Figure 4, it is evident that the surface current distribution of mode 4 in almost every point is stronger than the surface current distribution of mode 5 except some points where the surface current distribution of mode 5 is stronger than that of mode 4. Basically, it is obvious from the figure that there are very negligible points with equal current distribution. So, it will be possible to obtain optimum CP radiation performance by exciting these two modes simultaneously.
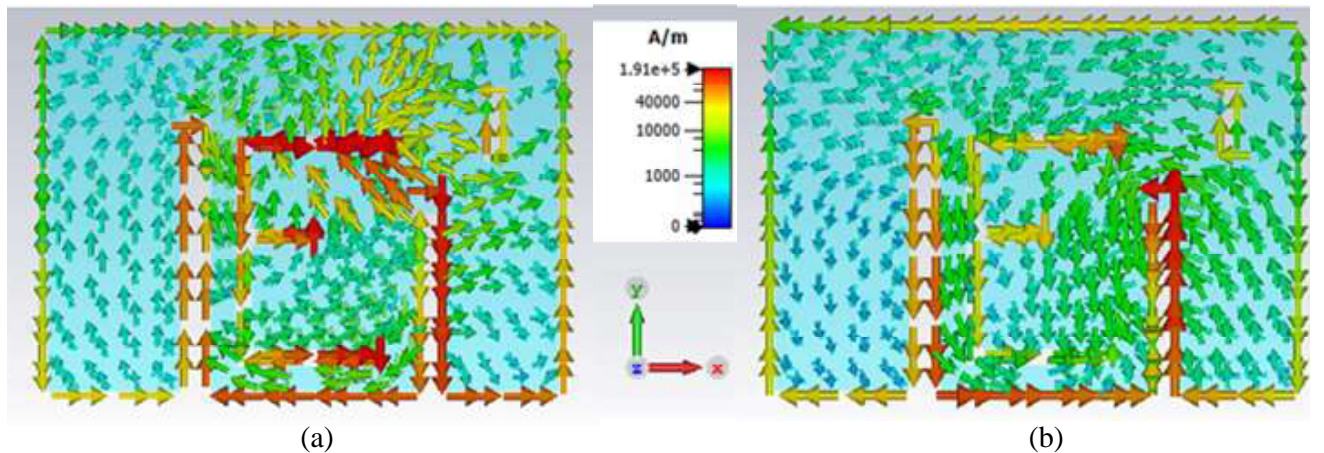

(a)   (b)

Figure 4. Modal current distribution curves (modes 4 and 5) at 1.11 THz of the proposed OTA. (a) Mode 4. (b) Mode 5.

4. PARAMETRIC STUDY

As per the authors' knowledge, this is the first time in a literature where CMA is utilized for parametric study, as this analysis helps to obtain high computational efficiency by reducing the optimization time significantly [50]. The change of each parameter causes some changes in all of the resonant characteristics. However, some of these changes are more significant (L_1 and $L_1 - X_1$, L_2 and $L_2 + X_2$, a, W_S, and E_3) than others (h, E_1, E_2, L_{SI}, E_S, W_{SI}) in the considered range which lead hypotheses regarding the interaction of antenna geometry and behavior. This interaction will be explored in this section. It is mentioned here that optimization is done by considering all five modes along with MS_n, α_n, λ_n. But for the ease of simplicity, only the significance of mode 4 and mode 5 in terms of MS_n and α_n is discussed here, as they are the modes to be excited to obtain CP antenna.

Figure 5 shows the effect of change of patch slit length, L_1, and CNT cover slit length, ($L_1 - X_1$). The change of these parameters has significant effects on determining resonant frequency and AR. From the figures, it is seen that when L_1 and ($L_1 - X_1$) both are equal to 35 μm, there is no intersection between MS_n curves of mode 4 and mode 5, and these modes act as inductive and capacitive modes, respectively, as evident from α_n curves. But with the increase of both slits length to 40 μm, the inversion of modes takes place, i.e., mode 4 becomes capacitive mode, and mode 5 becomes inductive mode; MS_n of both the modes are equal at 1.13 THz and 1.21 THz. But at these frequencies the difference of α_n of the modes is not near 90°. So, it is not possible to get better AR performance by exciting these two modes at these frequencies. It is found that after creating difference in slits lengths of the cover and patch, i.e., $L_1 = 40$ μm and ($L_1 - X_1$) = 35 μm, the two modes cross each other at 1.11 THz and the angle between modal current and the tangential electric field on the surface, i.e., α_n reaches optimum value which helps to obtain better AR value when being excited properly.
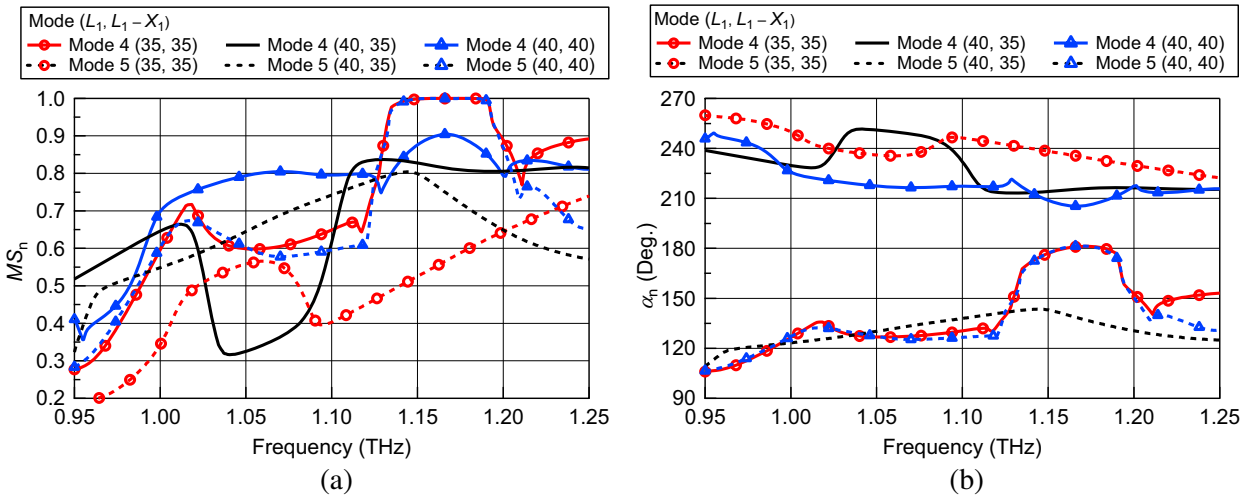

Figure 5. Effect of change of slit lengths, L_1 and ($L_1 - X_1$) (Slit-1) on MS_n and α_n. (a) Modal significance (MS_n). (b) Characteristic angle (α_n).

Figure 6 illustrates the effect of varying slits lengths, L_2 (patch) and ($L_2 + X_2$) (CNT cover) at Slit-2. It is observed that for equal length of cover and patch slits (53 μm and 59 μm), there are several frequencies with the same MS_n of mode 4 and mode 5. However, the difference of α_n between mode 4 and mode 5 is not near 90° at these frequencies. But by creating the difference in slots lengths, the values of MS_n become equal at 1.11 THz with optimum α_n. So it is possible to get better AR performance for these two modes at this frequency when excitation is provided.

Figure 7 presents the impact of change of 'a' on MS_n and α_n, where 'a' is the distance between Slit-2 and $\lambda/4$ transformer. During this investigation, $W_S = 6$ μm is kept fixed. It is observed that for $a = 16$ μm, there are two frequencies with the same MS_n, but the difference of α_n is not considerable to obtain CP performance at these frequencies. It is obvious that better performances in terms of both
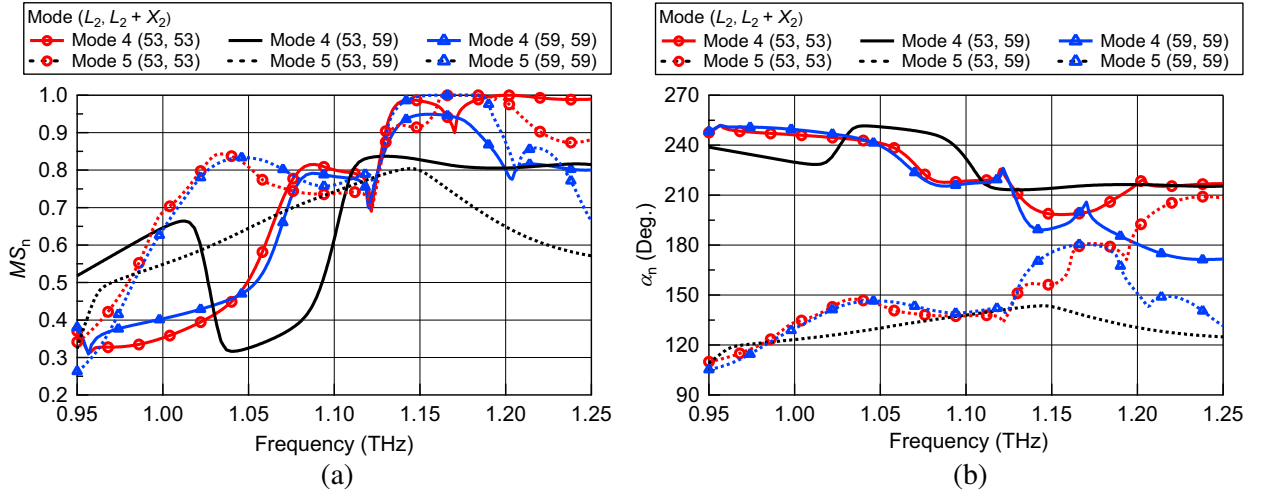
Figure 6. Effect of change of slit lengths, L_2 and $(L_2 + X_2)$ on MS_n and α_n. (a) Modal significance (MS_n). (b) Characteristic angle (α_n).
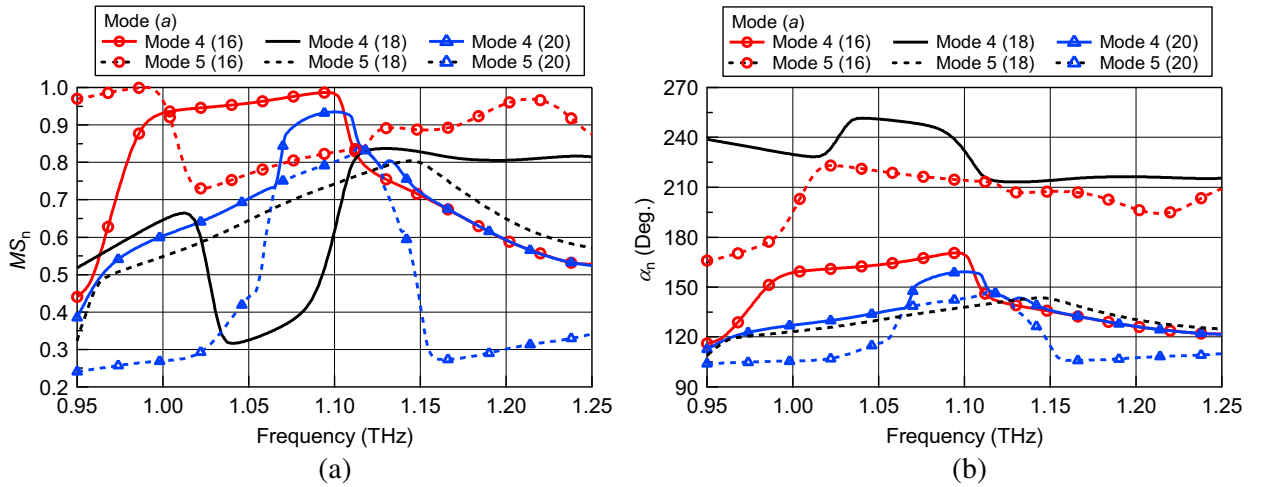

Figure 7. Impact of 'a' on MS_n and α_n. (a) Modal significance (MS_n). (b) Characteristic angle (α_n).

MS_n and α_n is obtained for $a = 18\,\mu\text{m}$ at 1.11 THz. If 'a' is increased further ($a = 20\,\mu\text{m}$), the frequency is shifted from 1.11 THz to 1.12 THz, and MS_n is increased too, but inversion of modes takes place, and both the modes become inductive modes. So it will not be possible to get better AR performance at 1.12 THz than that obtained for $a = 18\,\mu\text{m}$ at 1.11 THz.

Figure 8 shows the effect of varying the width of Slit-2 (W_S). For this analysis, slit widths of the ITO patch and CNT cover are changed equally, and other parameters are kept constant. It is visible that better AR performance is possible to obtain for $W_S = 6\,\mu\text{m}$ as mode 4 and 5 intersect at 1.11 THz with optimum α_n. For widening or reducing the slots width, the AR performance degrades significantly in terms of both MS_n and α_n as the two modes do not intersect with each other for any other frequencies except 1.02 THz and 1.08 THz. But at these frequencies, the values of MS_n are less than the value obtained for $W_S = 6\,\mu\text{m}$ at 1.11 THz, i.e., both modes are less significant at these frequencies.

Figure 9 presents the influence of the lower arm of the E-shaped slot by changing the length, E_3. It is obvious that modes 4 and 5 have the same MS_n at 1.11 THz for $E_3 = 25\,\mu\text{m}$. For decreasing the slot length, it is seen that there are no frequencies with the same MS_n value of mode 4 and mode 5, and both modes become inductive modes and store only magnetic field energy as evident from α_n curves.
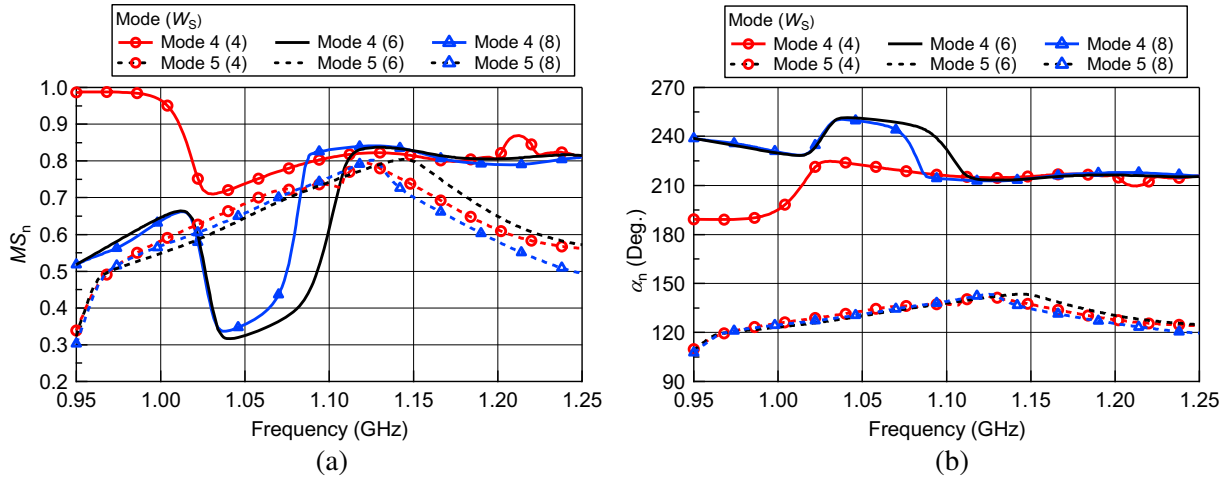
Figure 8. Effect of change of slit-2 width, W_S on MS_n and α_n. (a) Modal significance (MS_n). (b) Characteristic angle (α_n).
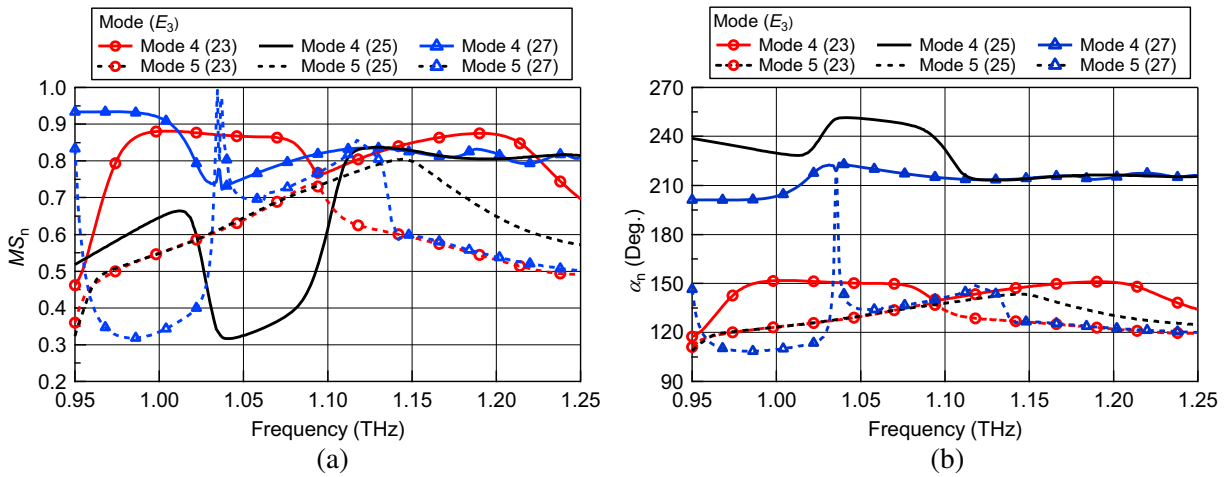

Figure 9. Influence of slot length, E_3 on MS_n and α_n. (a) Modal significance (MS_n). (b) Characteristic angle (α_n).

On the other hand, for increasing the slot length, it is seen that, at 1.04 THz, MS_n of both modes are the same. However, the difference of α_n is not near $90°$, even both modes become capacitive modes at this certain frequency. So for this value, it will not be possible to obtain CP performance by providing excitation.

5. RESULTS AND DISCUSSIONS

The simulation of the proposed antenna is done in CST MW Studio in frequency domain. An ITO based antenna without using CNT coating is also designed to visualize the improvement of performance of the proposed antenna due to using CNT coating. The reflection coefficient and radiation attributes are inquired in 0.95–1.25 THz. The reflection coefficient of the proposed transparent antenna along with ITO based antenna without CNT coating is depicted in Figure 10(a). From the depiction, it is observed that a reflection coefficient of less than -63 dB at 1.12 THz with fine wide 10-dB fractional BW of 22.32% is achieved for the proposed antenna. This high value of reflection coefficient signifies that an excellent impedance matching is obtained and ensures maximum radiation of the power supplied to
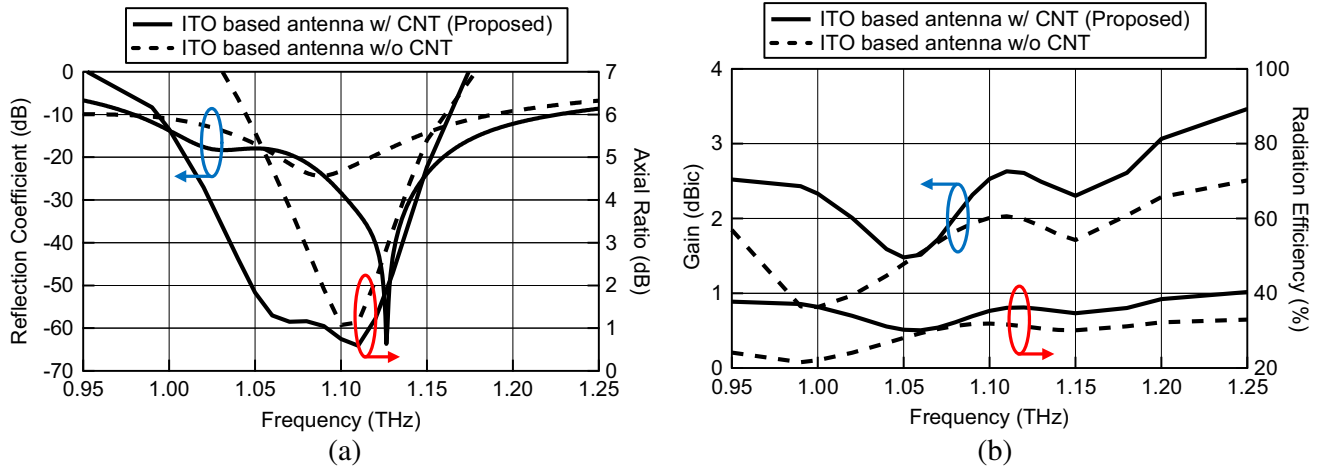
Figure 10. Simulated (a) reflection coefficient along with AR and (b) gain with radiation efficiency of the OTA w/ and w/o CNT.

the antenna. This result also confirms the right placement of the feed line on the patch for resonant frequency of 1.12 THz. For the ITO based antenna without CNT coating at resonance frequency of 1.09 THz, the reflection coefficient of 25 dB is achieved with 10-dB fractional BW of 21.80%.

The AR of the proposed antenna along with ITO based antenna without CNT coating is also plotted in Figure 10(a) to find the frequency range where the CP is achieved. From the curve, it is observed that at 1.11 THz, the obtained minimum AR is 0.58 dB for the proposed antenna which is less than the standard value of AR (< 3 dB) for CP antenna. A fine 3-dB AR BW of 105 GHz (9.66%) is achieved. This wide BW facilitates several advantages over conventional narrow ones, such as higher achievable data rates and increased immunity to interference due to lower spectral power density. This considerably high AR BW is obtained owing to two unequal parallel slits of E-shaped patch and CNT cover with unequal arms of an E-shaped slot embedded into the patch. The I-shaped slots embedded into both patch and cover also contribute to increased AR BW. For the ITO based antenna without CNT coating, the obtained minimum AR is 1.00 dB at 1.10 THz with a 3-dB AR BW of 50 GHz.

Figure 10(b) depicts the gain of the proposed ITO based antenna. It is seen that a reasonable gain of 2.61 dBic is obtained at a frequency of 1.12 THz. Though the gain obtained is sufficient for wireless communication, it is not so high due to the high resistivity of ITO and the extra slots integrated into the patch and cover. For ITO based antenna without CNT coating, a gain of 1.85 dBic is obtained at a frequency of 1.09 THz. From this figure, it can be concluded that there is a significant improvement of gain obtained due to the application of highly conductive CNT coating over highly resistive ITO patch.

The radiation efficiency of the proposed antenna and ITO based antenna without CNT is also illustrated in Figure 10(b). A radiation efficiency of 36.2% is achieved at 1.12 THz for the proposed antenna while for ITO based antenna without CNT coating, an efficiency of 32% at 1.09 THz is obtained. Due to low conductivity of ITO, the efficiency of ITO based antenna without CNT is low. It is evident that the efficiency is increased significantly for the proposed antenna due to the use of highly conductive CNT coating over the patch. Transparent antennas having efficiency of more than 30% is suitable for practical application [51]. As the efficiency of the proposed antenna is more than 30% over the entire band, it is possible to use this antenna in satellite applications by placing it on optical displays or heat reflecting transparent mirrors.

Figure 11 represents the far field radiation pattern of the proposed antenna in the x-z and y-z planes, respectively. The pattern is plotted at a frequency of 1.11 THz where AR is minimum. From the curve it is observed that radiation of the antenna is LHCP, and excellent cross polarization suppression of more than 32 dB is achieved. It ensures the reduction of loss of energy in the unintended direction. Due to unsymmetrical structure, maximum radiation is shifted to 30°, and maximum gains in x-z and y-z planes at 1.11 THz are 4.7 dBic and 5.52 dBic, respectively. On the other hand, gains of 2.61 dBic and 2.91 dBic in x-z and y-z planes are correspondingly achieved at $\theta = 0°$.
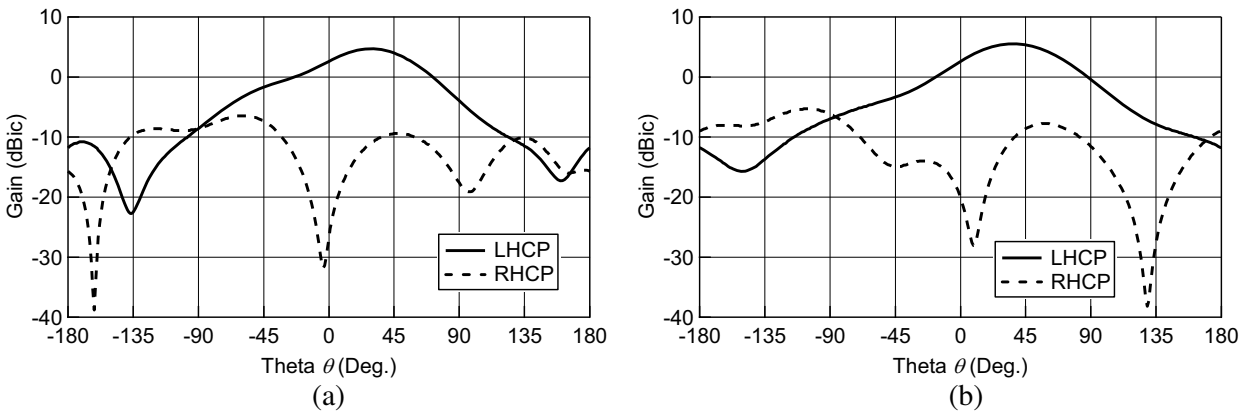
Figure 11. Far field CP radiation pattern of the proposed CP OTA in (a) x-z plane and (b) y-z plane at 1.11 THz.

6. BENEFITS AND COMPARISONS

In conventional antenna design process, parametric study is done by "cut and try" [49] method which takes a lot of time for optimization. But in this design, parametric study is done by using CMA in integral equation solver. This process helps to reduce the optimization time significantly. Besides, CMA helps to detect the CP generation modes as well as explain CP generation mechanism clearly which is ambiguous in traditional design process. The proposed antenna is an LHCP antenna. More importantly, it is possible to obtain RHCP sense by mirroring the design [31]. It is to be noted that almost similar performance in terms of reflection coefficient, AR, gain, and radiation efficiency is obtained after mirroring the design. Due to the high resistivity as well as slots embedding, the performance of the ITO based antenna without CNTis degraded which is overcome significantly by using CNT coating over the patch in the proposed antenna.

Table 2 represents a comparison of radiation performance of the presented work with some earlier standard researches on OTAs. It is evident that 10-dB impedance BW of the proposed antenna is 250 GHz which is much wider than the BW of reference cases mentioned in the table. It is also found that the 3-dB AR BW of the proposed antenna is 105 GHz which ensures better CP performance.

Table 2. Performance comparison of the presented work with some earlier OTAs.

Antenna	Patch Material	Freq. (THz)	10-dB Imp. BW (%, GHz)	3-dB AR BW (%, GHz)	Gain (dBi or dBic)	Polarization Sense
[5]	FTO	0.75	13.12, 99	-	2.82	LP
[12]	ITO	0.75	9.54, 72	-	3.31	LP
[12]	FTO	0.75	11.49, 86	-	2.10	LP
[13]	ITO	0.75	11.73, 87	-	3.80	LP
[14]	Graphene	6.00	12.83, 770	-	3.27	LP
[18]	Cu with quartz glass	0.024	6.7, 1.60	1.87, 0.50	4.00	RHCP
[19]	AgHT-4	0.0058	59.48, 3.45	13.7, 0.80	0.92	RHCP
Proposed	CNT coated ITO	1.12	22.32, 250	9.66, 105	2.61	LHCP

Though the gain of the proposed antenna is not so high, it is still competitive with other reference antennas. Finally, it is evident that wide 3-dB AR BW along with reasonable gain makes the proposed antenna suitable for various wireless applications.

7. CONCLUSION

In this paper, a transparent CNT coated ITO based E-shaped antenna with wideband performance has been proposed. CMA is carried out to optimize the antenna structure which helps to reduce the optimization time significantly compared to conventional optimization technique. An E-shaped slot and an I-shaped slot are embedded to achieve the CP. Moreover, CNT is used as a cover of the patch which helps to improve the gain and 3-dB AR BW significantly. The cross polarization suppression of more than 32 dB is achieved which ensures better radiation performance of the antenna. Sufficient gain, wide 3-dB ARBW along with high cross polarization suppression make this simple, compact transparent antenna fit for various wireless communication applications.

CONFLICT OF INTEREST

The authors declare no potential conflict of interest.

REFERENCES

1. He, Y., Y. Chen, L. Zhang, S.-W. Wong, and Z. N. Chen, "An overview of terahertz antennas," *China Communications*, Vol. 17, No. 7, 124–165, Jul. 2020.

2. Jamshed, M. A., A. Nauman, M. A. B. Abbasi, and S. W. Kim, "Antenna selection and designing for THz applications: Suitability and performance evaluation: A survey," *IEEE Acc.*, Vol. 8, 113246–113261, Jun. 2020.

3. Lee, S., M. Choo, S. Jung, and W. Hong, "Optically transparent nano-patterned antennas: A review and future directions," *Appl. Sci.*, Vol. 8, No. 6, May 2018.

4. Zhou, Y. and R. Azumi, "Carbon nanotube based transparent conductive films: Progress, challenges, and perspectives," *Science and Technology of Advanced Materials*, Vol. 17, No. 1, 493–516, Sep. 2016.

5. Anand, S., M. S. Darak, and D. S. Kumar, "Investigation of fluorine-doped tin oxide based optically transparent E-shaped patch antenna for terahertz communications," *Proc. AIP Conf.*, 430–436, Feb. 2014.

6. Simons, R. N. and R. Q. Lee, "Feasibility study of optically transparent microstrip patch antenna," *IEEE Antennas Propag. Soc. Int. Symp. 1997, Dig.*, 2100–2103, Jul. 1997.

7. Mias, C., C. Tsakonas, N. Prountzos, et al., "Optically transparent microstrip antennas," *IEE Colloq. Antennas Automotives*, 8, IEE, Feb. 2000.

8. Guan, N., H. Furuya, K. Himeno, K. Goto, and K. Ito, "Basic study on an antenna made of a transparent conductive film," *IEICE Trans. Commun.*, Art no. E90-B(9), Sep. 2007.

9. Yasin, T., R. Baktur, and C. Furse, "A comparative study on two types of transparent patch antennas," *2011 XXXth URSI Gen. Assem. Sci. Symp.*, 1–4, IEEE, Aug. 2011.

10. Song, H. J., T. Y. Hsu, D. F. Sievenpiper, H. P. Hsu, J. Schaffner, and E. Yasan, "A method for improving the efficiency of transparent film antennas," *IEEE Antennas Wirel. Propag. Lett.*, Vol. 7, 753–756, Oct. 2008.

11. Saberin, J. R. and C. Furse, "Challenges with optically transparent patch antennas," *IEEE Antennas Propag. Mag.*, Vol. 54, 10–16, Jul. 2012.

12. Thampy, A. S. and S. K. Dhamodharan, "Performance analysis and comparison of ITO- and FTO-based optically transparent terahertz U-shaped patch antennas," *Phys. E Low-Dimensional Syst. Nanostructures*, Vol. 66, 52–58, Feb. 2015.

13. Anand, S., M. S. Darak, and D. Sriram Kumar, "Investigations on indium tin oxide based optically transparent terahertz E-shaped patch antenna," *Adv. Intell. Syst. Comput.*, Vol. 264, 195–202, 2014.

14. Thampy, A. S., M. S. Darak, and S. K. Dhamodharan, "Analysis of graphene based optically transparent patch antenna for terahertz communications," *Phys. E Low-Dimensional Syst. Nanostructures*, Vol. 66, 67–73, Feb. 2015.

15. Desai, A., T. Upadhyaya, J. Patel, R. Patel, and M. Palandoken, "Flexible CPW fed transparent antenna for WLAN and sub-6 GHz 5G applications," *Microw. Opt. Technol. Lett.*, Vol. 62, No. 5, 2090–2103, Feb. 2020.

16. Desai, A., T. Upadhyaya, M. Palandoken, J. Patel, and R. Patel, "Transparent conductive oxide-based multiband CPW fed antenna," *Wireless Personal Communications*, Vol. 113, 961–975, Apr. 2020.

17. Desai, A., T. Upadhyaya, and R. Patel, "Compact wideband transparent antenna for 5G communication systems," *Microw. Opt. Technol. Lett.*, Vol. 61, No. 3, 781–786, Mar. 2019.

18. Dao, Q. H., T. J. Cherogony, and B. Geck, "Optically transparent and circularly polarized patch antenna for K-band applications," *2016 IEEE Ger. Microw. Conf.*, 247–250, Mar. 2016.

19. Wahid, W. I., M. R. Kamarudin, M. Khalily, and T. Peter, "Circular polarized transparent antenna for 5.8 GHz WLAN applicatons," *Progress In Electromagnetics Research Letters*, Vol. 57, 39–45, 2015.

20. Rahman, M. A., E. Nishiyama, and I. Toyoda, "A wideband dual-circularly polarized 2 × 1 array antenna using multi-layer substrate for compact structure," *Microw. Opt. Technol. Lett.*, Vol. 62, No. 1, 474–483, Sep. 2019.

21. Khidre, A., K. F. Lee, F. Yang, and A. Elsherbeni, "Wideband circularly polarized E-shaped patch antenna for wireless applications," *IEEE Antennas Propag. Mag.*, Vol. 52, No. 5, 219–229, Oct. 2010.

22. Rahman, M. A., E. Nishiyama, and I. Toyoda, "A polarization reconfigurable microstrip antenna employing dual-perturbation technique," *Progress In Electromagnetics Research M*, Vol. 69, 197–206, 2018.

23. Garbacz, R. and R. Turpin, "A generalized expansion for radiated and scattered fields," *IEEE Trans. Antennas Propag.*, Vol. 19, No. 3, 348–358, May 1971.

24. Harrington, R. F. and J. R. Mautz, "Theory of characteristic modes for conducting bodies," *IEEE Trans. Antennas Propag.*, Vol. 19, No. 5, 622–628, Sep. 1971.

25. Harrington, R., J. Mautz, and Y. Chang, "Characteristic modes for dielectric and magnetic bodies," *IEEE Trans. Antennas Propag.*, Vol. 20, No. 2, 194–198, Mar. 1972.

26. Tran, H. H., N. Nguyen-Trong, and A. M. Abbosh, "Simple design procedure of a broadband circularly polarized slot monopole antenna assisted by characteristic mode analysis," *IEEE Acc.*, Vol. 6, 78386–78393, Dec. 2018.

27. Zhang, Q., R. Ma, W. Su, and Y. Gao, "Design of a multimode UWB antenna using characteristic mode analysis," *IEEE Trans. Antennas Propag.*, Vol. 66, No. 7, 3712–3717, Jul. 2018.

28. Luo, Y., Z. N. Chen, and K. Ma, "Enhanced bandwidth and directivity of a dual-mode compressed high-order mode stub-loaded dipole using characteristic mode analysis," *IEEE Trans. Antennas Propag.*, Vol. 67, No. 3, 1922–1925, Mar. 2019.

29. Yan, Y., J. Ouyang, X. Ma, R. Wang, and A. Sharif, "Circularly polarized rfid tag antenna design for metallic poles using characteristic mode analysis," *IEEE Antennas Wireless Propag. Lett.*, Vol. 18, No. 7, 1327–1331, Jul. 2019.

30. Han, M. and W. Dou, "Compact clock-shaped broadband circularly polarized antenna based on characteristic mode analysis," *IEEE Acc.*, Vol. 7, 159952–159959, Nov. 2019.

31. Chowdhury, M. S. U., M. A. Rahman, M. A. Hossain, and A. T. Mobashsher, "A transparent conductive material based circularly polarized nano-antenna for THz applications," *Proc. 2020 IEEE Region 10 Symposium (TENSYMP)*, 754–757, Dhaka, Bangladesh, Jun. 2020.

32. Chen, Z., W. Li, R. Li, Y. Zhang, G. Xu, and H. Cheng, "Fabrication of highly transparent and conductive indium-tin oxidethin films with a high figure of merit via solution processing," *Langmuir*, Vol. 29, No. 45, 13836–13842, Oct. 2013.

33. Chisca, S., I. Sava, V. Musteata, and M. Bruma, "Dielectric and conduction properties of polyimide films," *CAS 2011 Proceedings (2011 International Semiconductor Conference)*, 253–256, Oct. 2011.

34. Wu, X., C. Shu, X. He, S. Wang, X. Fan, Z. Yu, D. Yan, and W. Huan, "Optically transparent and thermal-stable polyimide filmsderived from a semi-aliphatic diamine: Synthesis andproperties," *Macromol. Chem. Phys.*, Vol. 221, No. 5, 1–7, Mar. 2020.

35. Zhang, W., H. Xiong, S. Wang, M. Li, and Y. Gu, "Electromagnetic characteristics of carbon nanotube film materials," *Chinese Journal of Aeronautics*, Vol. 28, No. 4, 1245–1254, May 2015.

36. Kaskekla, A., et al., "Aerosol-synthesized SWCNT networks with tunable conductivity and transparency by a dry transfer technique," *Nano Lett.*, Vol. 10, No. 11, 4349–4355, Sep. 2010.

37. Dash, S. and A. Patnaik, "Material selection for THz antennas," *Microw. Opt. Technol. Lett.*, Vol. 60, No. 5, 1183–1187, May 2018.

38. Mansour, A. M., N. Shehata, B. M. Hamza, and M. R. M. Rizak, "Efficient design of flexible and low cost paper-basedinkjet-printed antenna," *Int. J. Antennas Propag.*, Vol. 2015, 1–6, Sep. 2015.

39. Paracha, K. N., S. K. A. Rahim, H. T. Chattha, S. S. Aljaafreh, S. U. Rehman, and Y. C. Lo, "Low-cost printed flexible antenna by using an office printer forconformal applications," *Int. J. Antennas Propag.*, Vol. 2018, 1–7, Feb. 2018.

40. Whittow, W. G., et al., "Inkjet-printed microstrip patch antennas realized on textile for wearable applications," *IEEE Antennas Wirel. Propag. Lett.*, Vol. 13, 71–74, Jan. 2014.

41. Labiano, I. I. and A. Alomainy, "Flexible inkjet-printed graphene antenna on Kapton," *Flex Print Electron.*, Vol. 6, 1–8, Jun. 2021.

42. Kanso, A., et al., "Design and fabrication of EBG and CWP antennas using inkjet printing technology," *Microw. Opt. Technol. Lett.*, Vol. 55, No. 7, 1520–1526, Jul. 2013.

43. Kirsch, N. J., N. A. Vacirca, T. P. Kurzweg, A. K. Fontecchio, and K. R. Dandekar, "Performance of transparent conductive polymer antennas in a MIMO ad-hoc network," *2010 IEEE 6th Int. Conf. Wireless and Mobile Computing, Networking and Commun.*, 9–14, Oct. 2010.

44. ITO ink for transparent conductive films, https://product.statnano.com/product/9087/ito-ink-for-transparent-conductive-films, accessd on 30 Oct. 2021.

45. Gilshtein, E., et al., "Inkjet-printed conductive ITO patterns for transparent security systems," *Adv. Mater. Technol.*, Vol. 5, No. 9, 1–6, Sep. 2020.

46. CNT conductive ink, https://www.nanoshel.com/product/cnt-conductive-ink, accessd on 30 Oct. 2021.

47. Elwi, T. A., H. M. Al-Rizzo, D. G. Rucker, E. Dervishi, Z. Li, and A. S. Biris, "Multi-walled carbon nanotube-based RF antennas," *Nanotechnology*, Vol. 21, No. 4, 1–10, Jan. 2010.

48. Wakatsuki, A., Y. Muramoto, and T. Ishibashi, "Development of terahertz-wavephotomixer module using a uni-traveling-carrier photodiode," *NTT Technical Review*, Vol. 10, No. 2, 1–7, Feb. 2012.

49. Cabedo-Fabres, M., E. Antonino-Daviu, A. Valero-Nogueira, and M. F. Bataller, "The theory of characteristic modes revisited: A contribution to the design of antennas for modern applications," *IEEE Antennas Propag. Mag.*, Vol. 49, 52–68, Oct. 2007.

50. Chen, Y. and C. F. Wang, *Characteristic Modes*, John Wiley & Sons, Inc., Hoboken, NJ, 2015.

51. Yasin, T., R. Baktur, and C. Furse, "A study on the efficiency of transparent patch antennas designed from conductive oxide films," *2011 IEEE Int. Symp. Antennas Propag.*, 3085–3087, Jul. 2011.